Numerical and Experimental Study on the Pressure Distribution in a Volute of High-Speed Centrifugal Fan with Impeller- Volute interaction

Dr.Muthana K. Aldoory
College of Engineering, Kirkuk University

Ahmed A. Ali
College of Engineering, Diyala University

ABSTRACT

This paper shows a numerical simulation in capturing the dynamic and static pressure effects inside a centrifugal fan due to the impeller-volute interaction. The fan used in this study is a single-stage machine with an unshrouded impeller and external volute. Three volute tongue designs were investigated. Volute C had a full tongue and did not allow any flow recirculation. Volute B had a reduced tongue length thereby opening the recirculation port. Finally the tongue of volute A had a rounded leading edge to make it less sensitive to off-design flow conditions. For the numerical simulation, the viscous Navier-Stokes equations are handled with unstructured grid and the relative reference frames technique is applied to take into account the impeller-volute interaction. The data obtained allow the analysis of the main phenomena existent in these fans, such as: pressure changes in the volute for different flow rates and the secondary flow generated in the volute due to the width change between the impeller and the volute. Numerical results are compared with the experimental pressure data measured in the volute and agreement is found show that at low flow rates ,the volute decelerates the airflow leading to an increase in pressure throw the volute. At these low flow rates separation or flow unsteadiness can occur from the underside of the tongue and the strength of the instability increased when the mass flow rate was reduced further. The pressure fluctuation for various mass flow rates is a non-periodical nature and it is manifest as the broad band components in higher level of random frequency (up to nearly 500 Hz).This investigation concentrates on the measurement of the flow characteristic in the volute casing and the volute tongue configuration.

KEYWORDS Flow in volute, Centrifugal fan, volute tongue

دراسة نظرية وعملية على توزيع الضغط للمجرى الحلزوني لمروحة طرد مركزية ذات سرعة عالية مع تداخل الدافعة الحلزونية

د. مثنى خالص الدوري
كلية الهندسة / جامعة كركوك

أحمد علي
كلية الهندسة / جامعة ديالى

الخلاصة

يستعرض البحث التمثل العددي لحساب ضغط الهواء الديناميكي و الساكن في داخل المجمع (volute) لدافعة الهواء كنتيجة للتأثير المتبادل بين المروحة (impeller) و المجمع. دافعة الهواء المستخدمة في هذا الدراسة ذات مرحلة واحدة و المروحة من النوع المفتوح و المجمع خارجي. تم دراسة ثلاث أنواع من نتوء لسان (tongue) المجمع ، نوع C: لسان بطول كامل، لايسمح للهواء بالدوران في داخل المجمع.نوع B: لسان بطول غير كامل، يسمح لبعض الهواء بالدوران داخل المجمع ونوع A : لسان بنهاية مستديرة و حسب التصميم الأساسي لدافعة الهواء ليكون أقل حساسية للتشغيل خارج ظروف التصميم.

لغرض تمثيل الجريان استخدمت معادلات Navier- Stokes مع الأخذ بنظر الاعتبار لزوجة الهواء. الوصف الشبكي للمجمع من نوع غير المهيكل و ذو إطار مرجعي نسبي عند الأخذ بنظر الاعتبار للتأثير المتبادل ما بين المروحة و المجمع على خصائص الجريان. البيانات المستحصلة من هذا التمثيل استخدمت لتحليل ظاهرة طبيعة الجريان من حيث تغيير الضغط في المجمع كنتيجة لتغيير معدل جريان الهواء من الدافعة. استدلت النتائج إلى حدوث جريان ثانوي في المجمع بسبب وجود المسافة الفاصلة بين المروحة و المجمع. تم مقارنة النتائج العددية مع نتائج التجارب العملية و حصول التوافق بينهما. وقد بينت التجارب كذلك ان المجمع يعمل على تباطأ سرعة الهواء و زيادة في الضغط. عند معدلات الجريان الواطئة ويحصل عدم استقرار للجريان تحت منطقة نتوء اللسان و يزداد عدم الاستقرار عند الاستمرار في خفض معدلات الجريان. التذبذب في ضغط الهواء في المجمع ذو طبيعة عشوائية و يغطي طيف التذبذب مدى واسع و لغاية 500 Hz .

Received: 19 – 6 - 2011 **Accepted: 28 –12 - 2011**

NOMENCLATURE

D,d = Diameter (m)	Z = Number of blades	Subscripts
P = Pressure (N/m^2)	Greek Symbols	1 = Entry to the impeller
Q = Volumetric rate(m^3/s)	B = Blade angle(degree)	2 = Exit from the impeller
$\dot{m}$ = Mass flow rate (kg/s)	Ø= Circumferential angle(degree)	i = Impeller
f = Frequency(Hz)	y_{rms} = Root mean square value of static pressure fluctuation ($^{rms\ value}/_{\frac{1}{2}\rho U^2}$)	
r = Radius(m)		
t = Blade thickness(m)		

INTRODUCTION

Flow in centrifugal machines produces a complex three-dimensional phenomenon involving turbulence, secondary flows, unsteadiness, etc. (Brennen, 1994)[1]. Moreover, the geometry is complex and asymmetric due to the volute shape. The relative movement between impeller and volute generates an unsteady interaction which affects not only the overall performance (flow structure, losses), but is also responsible for pressure fluctuations, Which are one of the most Important sources of vibration and hydraulic noise (Dong et al., 1997)[2] . impellers of centrifugal pumps with volute casings at operating in off-design conditions are subjected to some static radial thrust, due to the non-uniform distributions of pressure and moment flux around the impeller (Rolling et al., 1960)[3].

Some authors (Kaupert et al., 1999)[4] have measured the unsteady pressure field inside the impeller of a centrifugal pump using piezoresistive pressure transducers and a telemetry system. They found amplitudes particularly high at the trailing edge of the blades (pressure side) and relative values up to 35 percent of the pump head at off-design conditions. Another important contribution to the understanding of the unsteady pressure field in the near–tongue region of the volute has been reported by (Whitefield et al., 2000)[5]. They used Particle Tracking Velocimetry (PTV) complemented with pressure measurements to measure the velocity distribution vicinity of three volute tongues of centrifugal fan. It was found that separation eddy (swirling, reverse flow) exists down stream of the leading edge of the tongue and that the flow separation from the leading edge of the tongue was reduced by the design modifications.

Parrondo et al. (2000)[6] presented an experimental study on the unsteady pressure centrifugal pump with spiral volute casing to measure and analyze the static pressure and the fluctuating pressure field existing in the volute. The results show that the static pressure around volute is uniform for the best efficiency point, but it exhibits either a maximum for lower flow rates or a minimum for higher flow rates . The pressure amplitude is small in the best efficiency region, and it increases fast in the region just behind the tongue for low and high flow rates.

Both experimental and numerical approaches have been reported and have contributed to the understanding of the highly complex flow interactions that occur in a centrifugal volute. Hagelstein et al. (2000)[7] studied the flow in a centrifugal compressor volute. The measurements were carried out at the diffuser exit. Several peripheral positions in the volute at the different levels of stage performance were located to carry on the measurements. The flow at the diffuser exit results in a forced vortex – type secondary flow inside the volute with an increase of swirl velocity from the vortex center to the volute walls. The results were compared with those obtained using the numerical results and agreement is observed.

CFD (computational fluid dynamic) has proven to be a very useful tool in the analysis of the flow inside volute casing, both in design and performance prediction. Much research has been carried out in the last years and used different techniques. Croba et al. (1996)[8] used relative reference frames technique to solve the unsteady flow in the casing while Blanco et al. (2000)[9] and Gonza`laz et al. (2002)[10] used sliding mesh technique, which has been applied to turbo machinery flow. However, due to the difficulties of the task, most of studies have been carried out with strong simplifications of the problem either in the geometry or in the flow characteristics. Research is slowly tending toward more complete simulations.

The purpose of the present simulation is to show a numerical study of a centrifugal fan for three tongue configurations and for different mass flow rates taking into account the complex geometry and the turbulence of the flow. It has been done with the commercial software package, FLUENT 5.3. This code uses the finite volume method and the Navier-Stokes equations with the ability to handle unstructured grid, including relative reference frames and making unsteady calculations with moving meshes.

MODEL DESCRIPTION AND COMPUTATIONAL METHOD

Although predictions on the unsteady flow field are always valuable, numerical simulation of centrifugal fans is not easy due to the usual CFD difficulties: turbulence modeling, flow separation, boundary layer (Lakshminarayana, 1991), etc. Beside that, there are also specific problems, as:

- Extremely complex geometry: a great number of cells is needed and, due to skew ness, usually unstructured grids give better convergence than structured ones.
- Energy transfer is generated mainly by the centrifugal force in the impeller. A cascade simulation is not valid and these force source terms must be included in the equations of the moving zone.
- The interaction between impeller and volute requires an unsteady solution process. In addition, the blade position with respect to the volute tongue must be taken into account.

Fan, Geometry and Grid:

Geometrical discrimination of the centrifugal fan is made for the numeric treatment, and computational grid is generated using the FLUENT preprocessor Gambit. In a pre-step, the walls limiting the airflow space are separated to form the volute and some more auxiliary edges needed for forming inner faces for impeller are constructed in Gambit. This is helpful since the complete grid is built up as block-structured.

- Unstructured triangular cells are used to define the impeller zone and volute zone. Once the geometry is defined, the model is ready to be simulated. A view of the generated grid for three cases can be seen in Figure (1) while detail of surface between impeller and volute defines the grid interfaces (interior) needed for the relative rotation of the impeller. The moving reference frame technique provided by FLUENT allows relative motion of the impeller grid with respect to the volute during simulation. Grid faces do not need to be aligned on both sides. The impeller and volute grid for three cases is shown in Table (1).

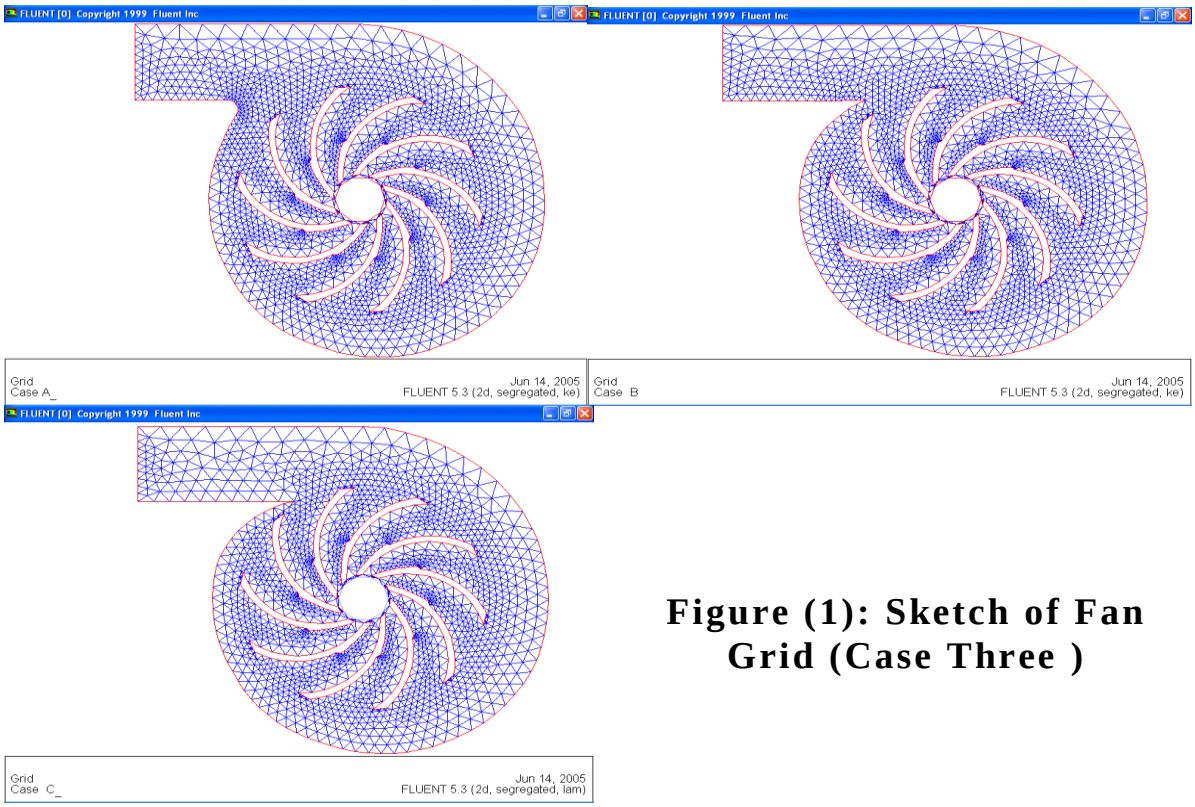

Figure (1): Sketch of Fan Grid (Case Three)

Table. 1: Detail of the Impeller and Volute Grid for Three Cases

Impeller zone	Case A	Case B	Case C
triangular cells	2569	2559	2563
Faces	3490	3475	3481
Volute zone	Case A	Case B	Case C
triangular cells	1567	1423	1243
Faces	2237	2021	1756
Node/case	2418	2341	2248

Mathematical Model.

The CFD approach allows for simplifications of the problem by considering :

- A fixed topology of the rotating wheel
- Centrifugal and Carioles forces in the wheel region
- The air as incompressible
- Turbulence as fully modeled

The steady state solution is obtained by solving Navier - Stokes equations with the implicit module of the CFD system, including the centrifugal force source in the impeller and the unsteady terms:

Mass $\nabla \cdot \mathbf{u} = 0$ .....(1)

Momentum $\rho \partial \mathbf{u} / \partial t + \rho(\mathbf{u} \cdot \nabla)\mathbf{u} - \nabla \tau + \nabla p = 0$ .....(2)

$$\bar{\nabla} = \left(\frac{\partial}{\partial x}\right)\bar{i} + \left(\frac{\partial}{\partial y}\right)\bar{j} + \left(\frac{\partial}{\partial z}\right)\bar{k}$$

with bold characters denoting vector quantities and the operator

$\overline{\nabla}$ are $(\partial/\partial x, \partial/\partial y, \partial/\partial z)$, $\mathbf{u}$ is the velocity vector, τ is the shear stress tensor and p is the pressure.

In the proposed CFD approach, two domains are considered, one is in the laboratory reference frame, and the other is calculated according to a rotating reference frame, i.e. centrifugal and Coriolis forces are added to Eq. (2):

$$\rho\partial\mathbf{u}/\partial t + \rho(\mathbf{u}\cdot\nabla)\mathbf{u} - \nabla\tau + \nabla p = -\rho\Omega\times\Omega\times(\mathbf{x}-\mathbf{x_o}) - 2\rho\Omega\times\mathbf{u} \qquad .(3)$$

Where x is the nodal coordinate vector; χ_o is the center of rotation; Ω is the angular velocity vector (that is, the angular velocity of the rotating frame). The above equations are solved using the finite element technique.

The turbulence behavior of the flow is simulated with the standard k- ε model. Turbulent intensity is not measured it is estimated to 5%. The pressure velocity couplings are calculated through the SIMPLE algorithm. Second order, upwind discretization have been used for convection terms and central difference schemes for diffusion terms.

Boundary Conditions:

The modeled boundary conditions are considered with more physical meaning for turbo machinery flow simulations, that is, total pressure at the inlet and a variable static pressure proportional to the kinetic energy at the outlet. The flow rate is changed by modifying the static pressure to kinetic energy ratio at the outlet condition, which simulates different closing positions of a valve. Some tests are carried out using a fixed flow rate at the inlet. Although it provides a better stability and faster convergence, this condition is found to be less physically correct, because the pressure obtained are quite different to the measured ones.

ANALYSIS OF NUMERICAL RESULTS.

The possibilities of the numerical simulation in the study of the flow inside a fan are wider than the experimental ones. In particular, results corresponding to the pressure distributions inside the impeller and near-tongue region and the flow in the volute are presented, and the unsteady calculation combined with the moving reference frame technique has proved to be a good tool to investigate the impeller – volute interaction.

Static Pressure inside the Fan:

The static pressure distribution on the impeller and fan casing on the mid-plane for three cases (A, B, C) for various mass flow rates are shown in Figure. (4). the static pressure rise through the fan is clearly seen in this figure, as are the radial pressure gradients.

The static pressure has a minimum value at the impeller eye, and around the impeller at the angular position about (Ø=95°) for case A and (Ø=40°) for cases B and C. This is because the tongue configuration affects the volute area (volute pressure) where volute pressure acts back on the impeller. The static pressure increases as the angular position around the volute increases except at position Ø=60° for case C.

In cases B and C, the higher pressures can be observed upstream of the leading edge of the volute tongue (stagnation point). Also, it can be seen that the pressure distribution over the suction pressure side of the blades is clearly appreciated, and the static pressure increases as the mass flow decreases.

Dynamic Pressure inside the Fan:

The resulting distributions, shown in Figure (3), characterize the dynamic behavior of the impeller-volute interactions on the mid-plane of the fan for three cases for different flow rates. From this figure, it can be seen that the dynamic pressure in the impeller increases as the radius ratio (radial gradients) increases, and the dynamic pressure magnitude is greater on the pressure side of the blade channel than on the suction side. On the suction side, a greater amount of disorder seems to exist which, could be caused by a localized recirculation zones formation in the impeller channels. The dynamic pressure within a fan impeller grows in magnitude as the mass flow rate is further departed from the lower flow rate region (0.0091kg/s , and non flow), and as the trailing edge (r/ri= 1) of a blade is approached.

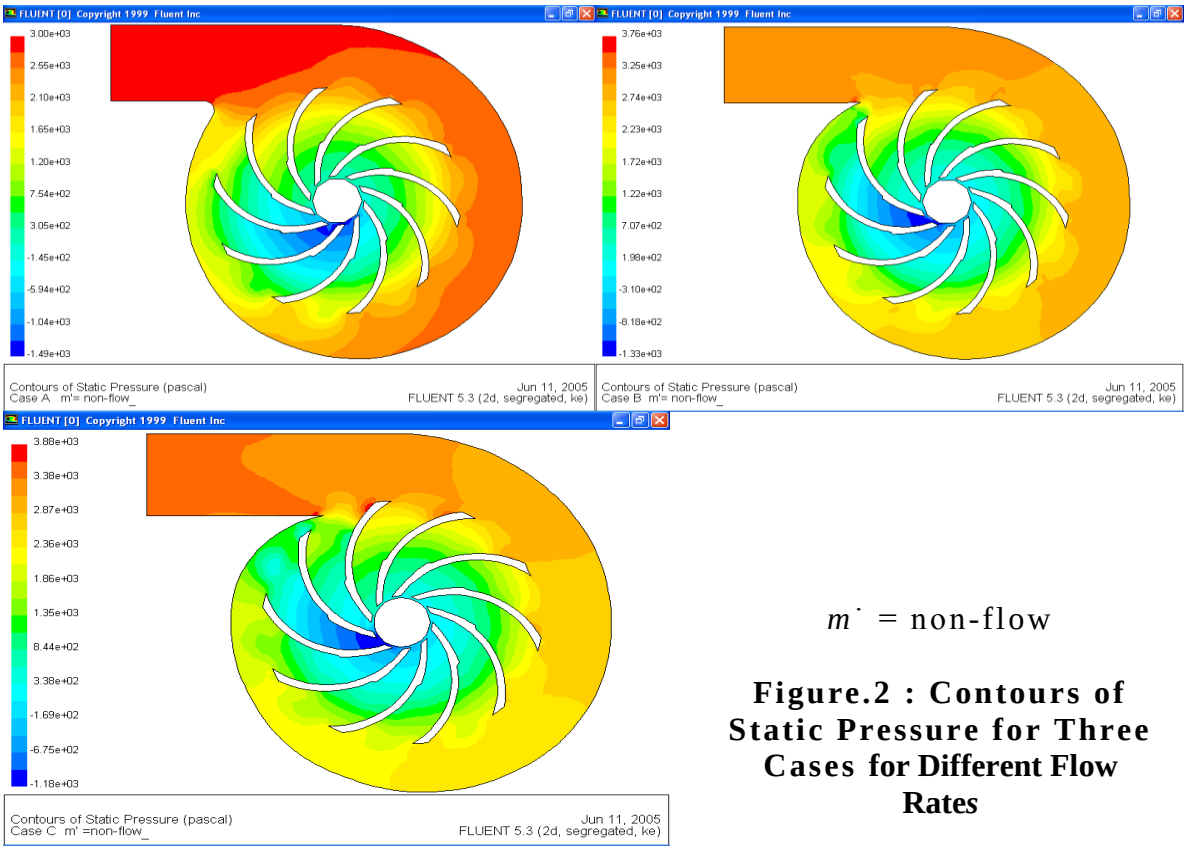

$\dot{m}$ = non-flow

Figure.2 : Contours of Static Pressure for Three Cases for Different Flow Rates

At nominal flow rate (i.e. $\dot{m}$=0.03046 kg/s), the dynamic pressure in the fan is large since the volute pressure distribution is small and uniform. At lower flow rate, the volute static pressure distribution rises; this manifests itself in the impeller as a dropping dynamic pressure after the blade passage rotates past a tongue (downstream of the tongue location about (Ø=90°) for case A and about (Ø=60°) for case B and C). Therefore, it can be seen how the tongue has no dynamic effect on flow rates near the nominal one, whereas it affects quite severely the dynamic pressure for off-design conditions.

The unsteady pressure field in the volute caused by the impeller rotation (i.e., jet-wake flow), is mostly steady in the impeller frame. Also, in this figure it can be observed that, the dynamic pressure has a maximum value in case A, at the angular position about (Ø=30°), in the blade passage. At the angular position opposite to the tongue in trailing edge of a blade in case B, and at the angular position opposite to the tongue in the blade passage in case C.

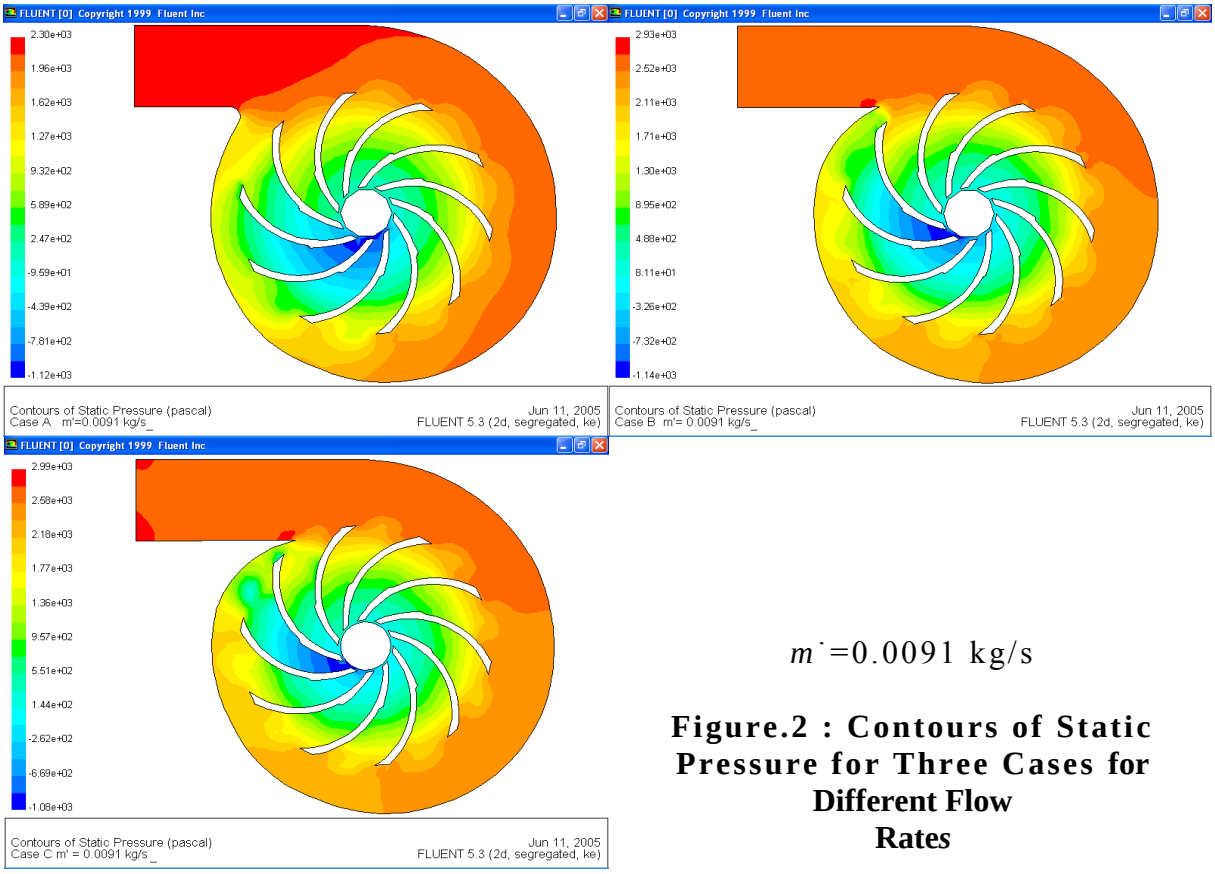

$\dot{m}$=0.0091 kg/s

Figure.2 : Contours of Static Pressure for Three Cases for Different Flow Rates

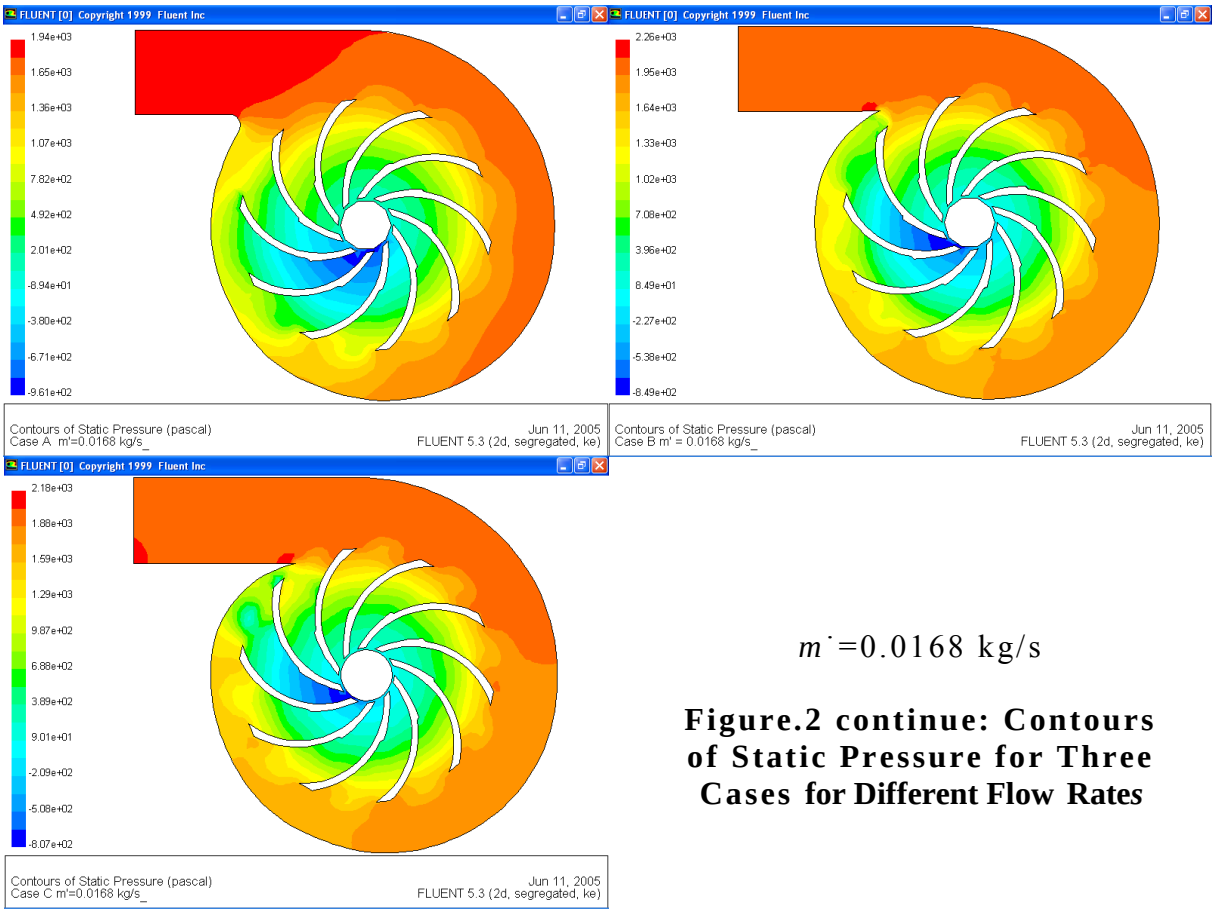

$\dot{m}$=0.0168 kg/s

Figure.2 continue: Contours of Static Pressure for Three Cases for Different Flow Rates

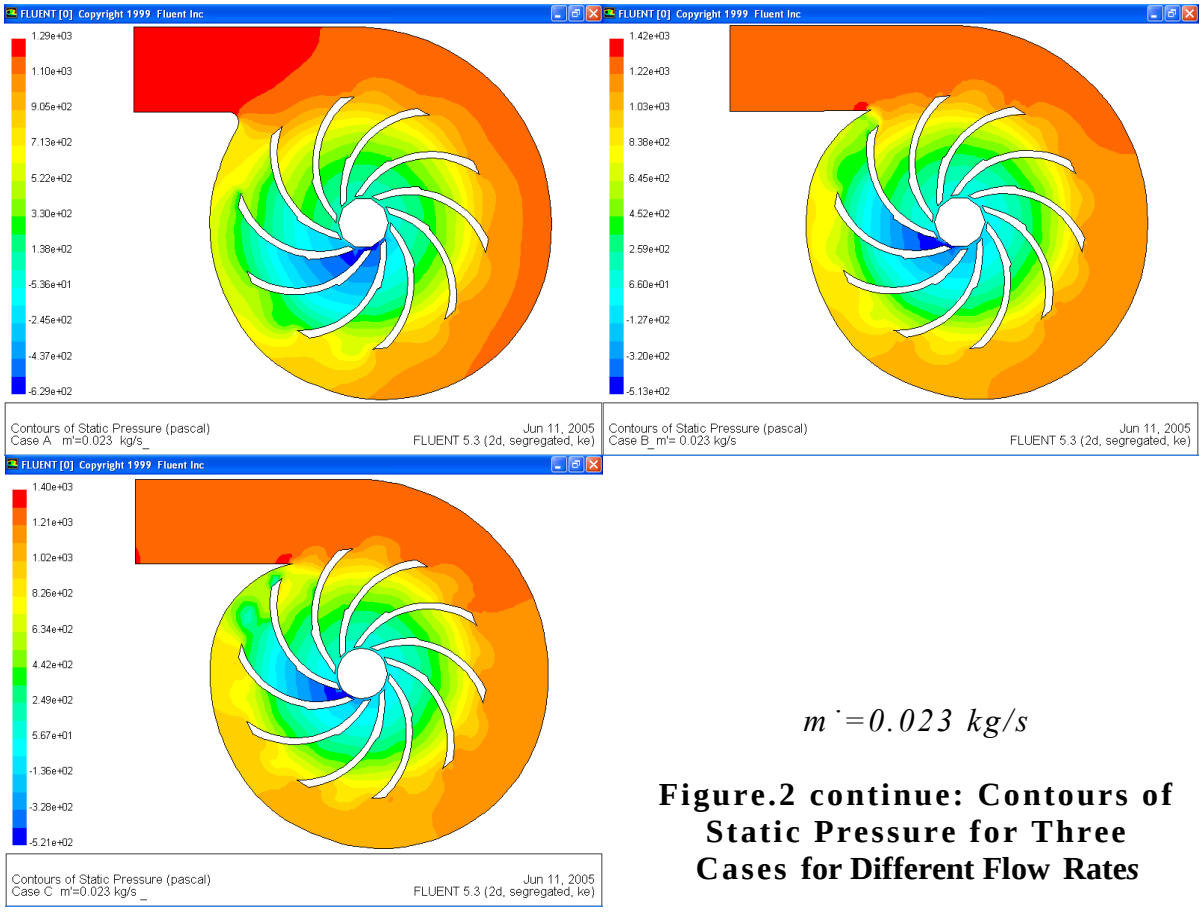

$\dot{m}=0.023\ kg/s$

Figure.2 continue: Contours of Static Pressure for Three Cases for Different Flow Rates

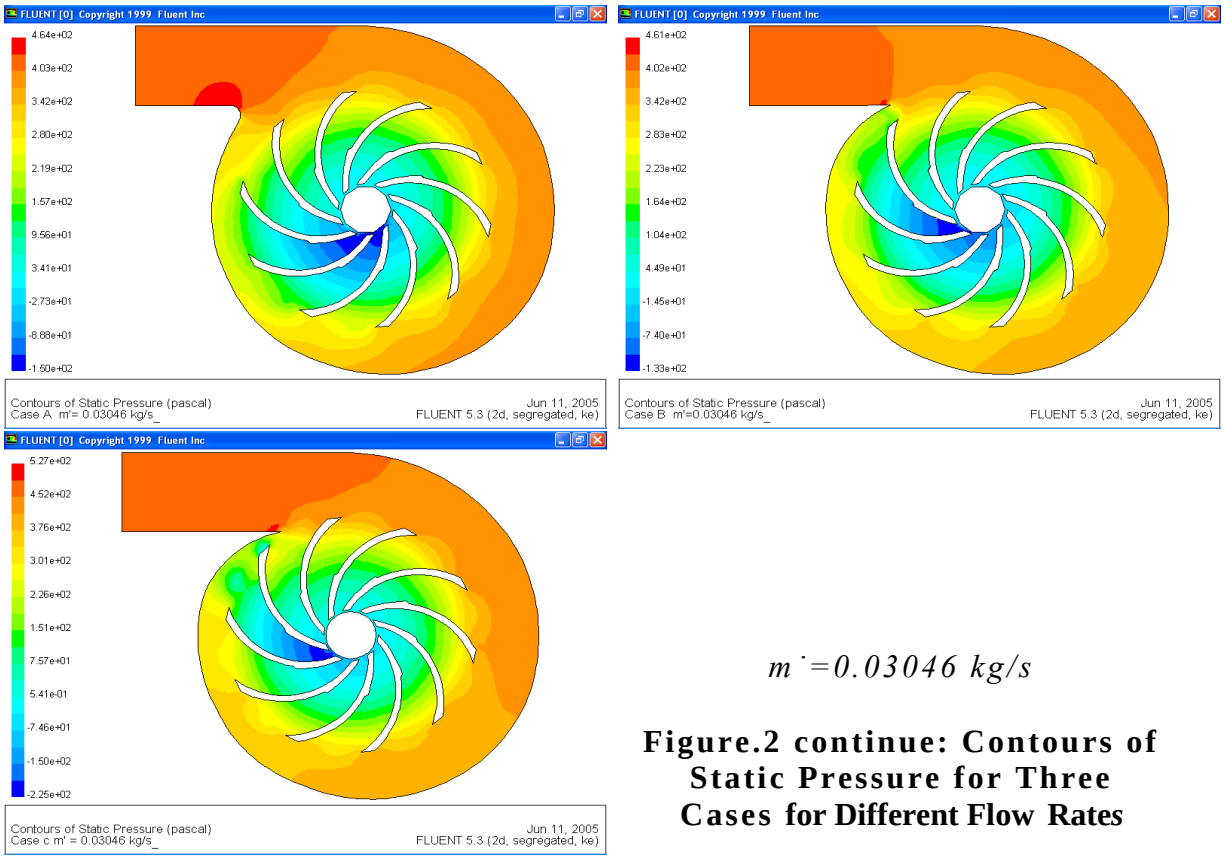

$\dot{m}=0.03046\ kg/s$

Figure.2 continue: Contours of Static Pressure for Three Cases for Different Flow Rates

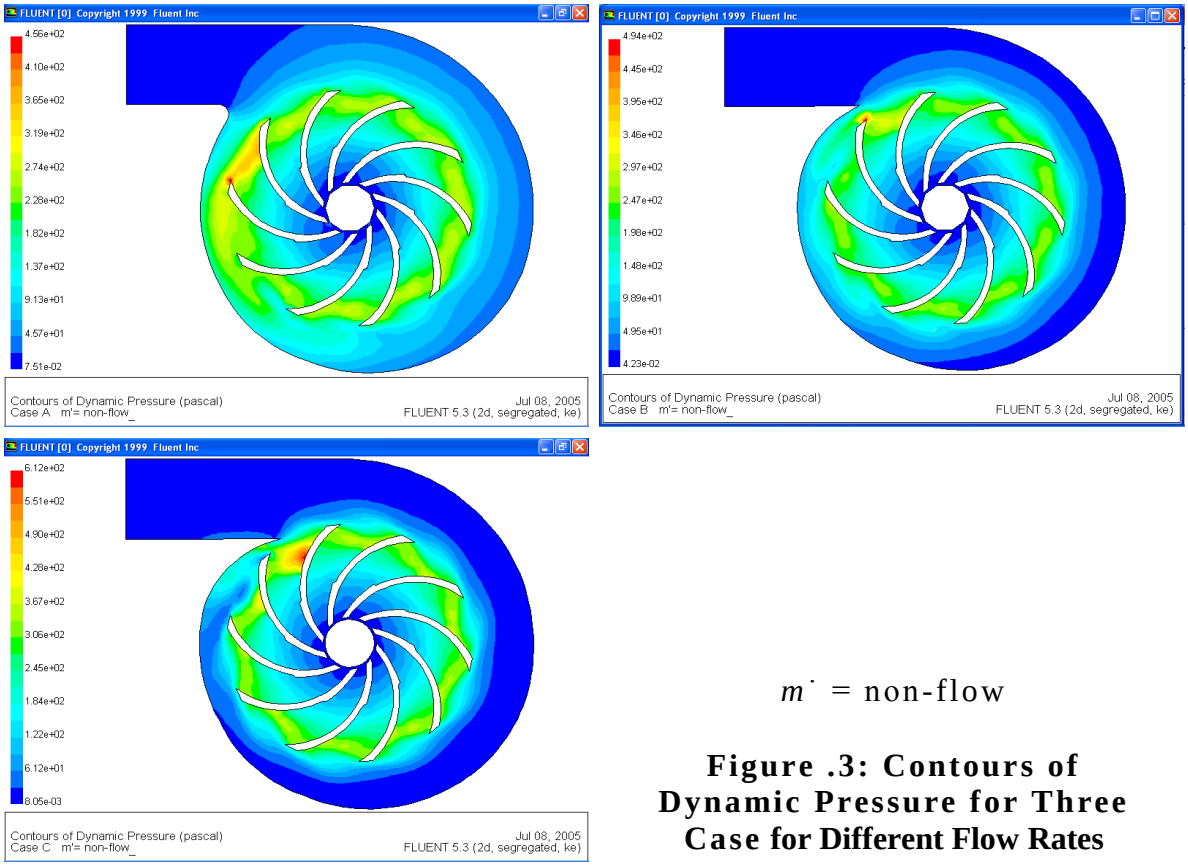

$\dot{m}$ = non-flow

Figure .3: Contours of Dynamic Pressure for Three Case for Different Flow Rates

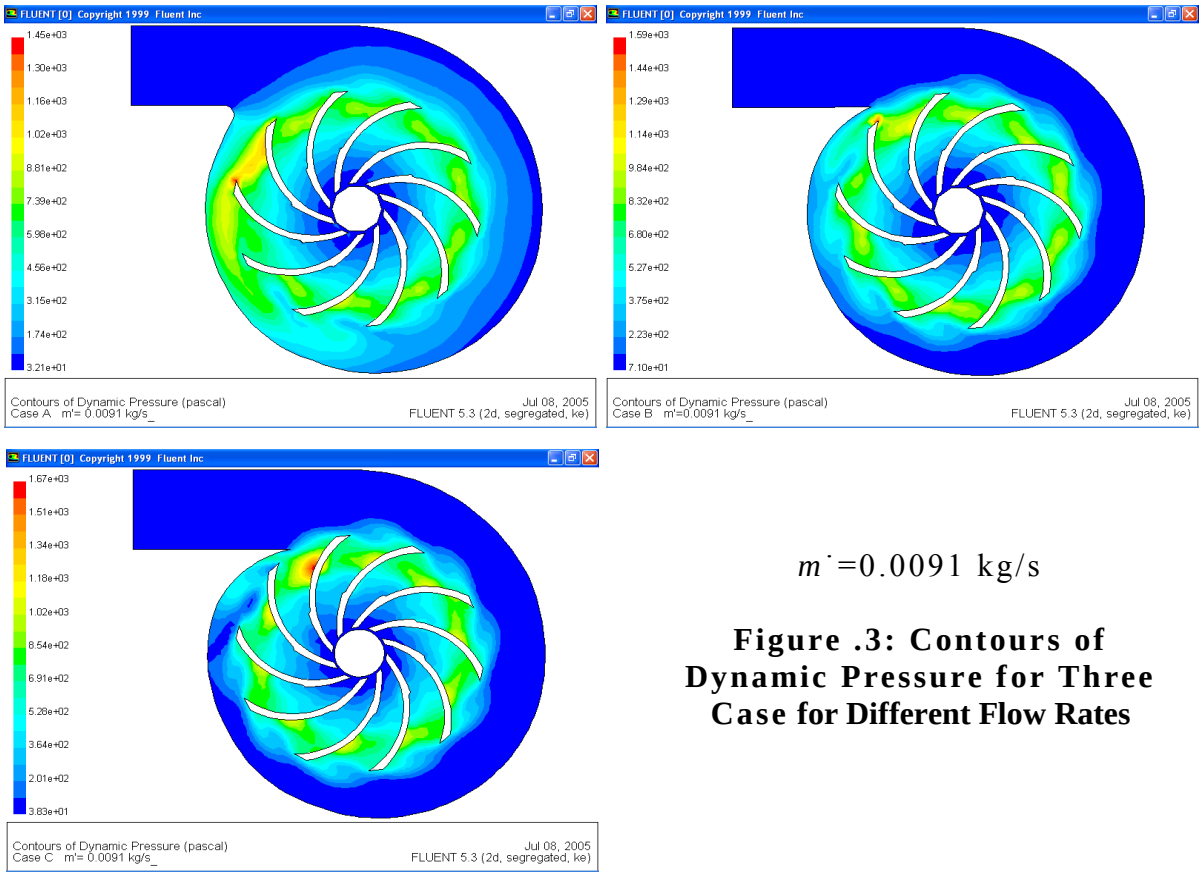

$\dot{m}$=0.0091 kg/s

Figure .3: Contours of Dynamic Pressure for Three Case for Different Flow Rates

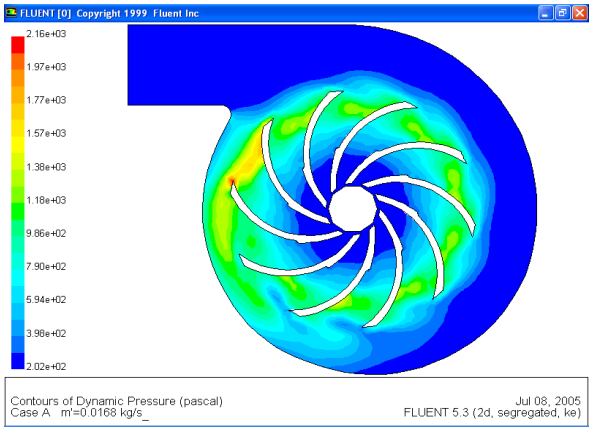

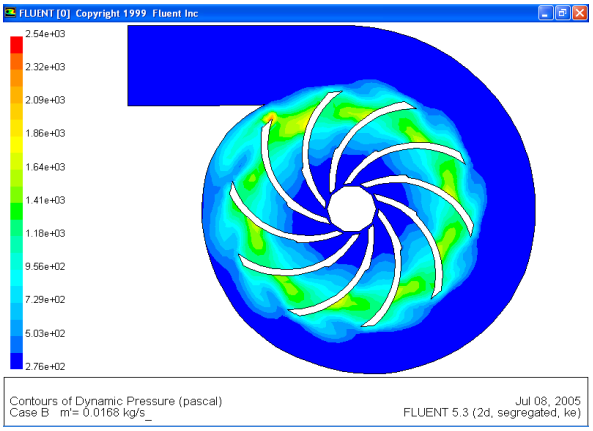

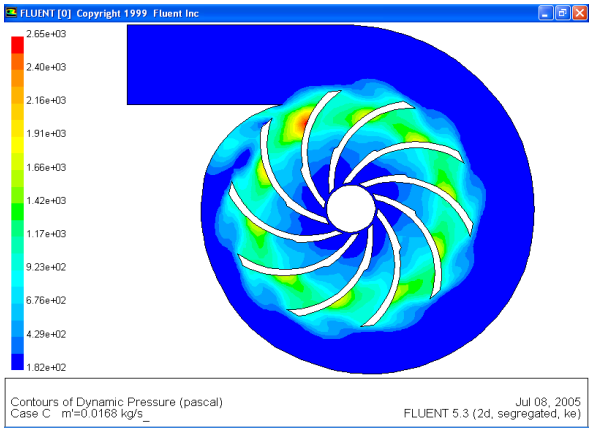

$\dot{m}=0.0168$ kg/s

Figure .3: Contours of Dynamic Pressure for Three Case for Different Flow Rates

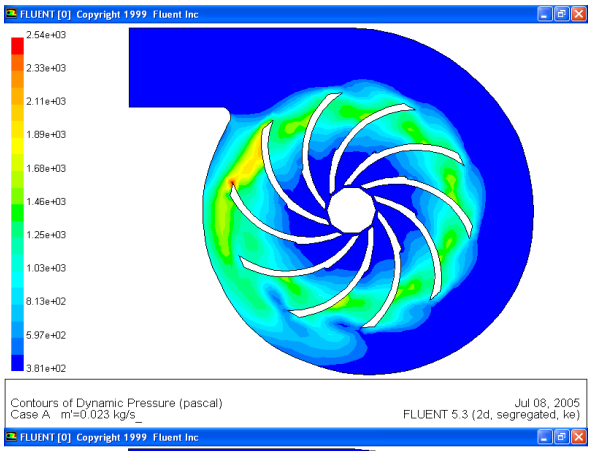

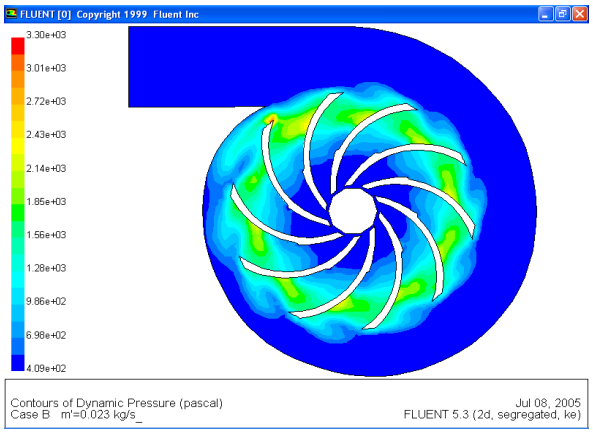

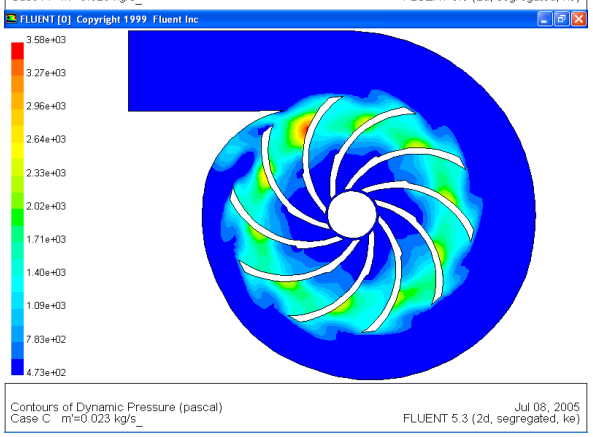

$\dot{m}=0.023$ kg/s

Figure .3: Contours of Dynamic Pressure for Three Case for Different Flow Rates

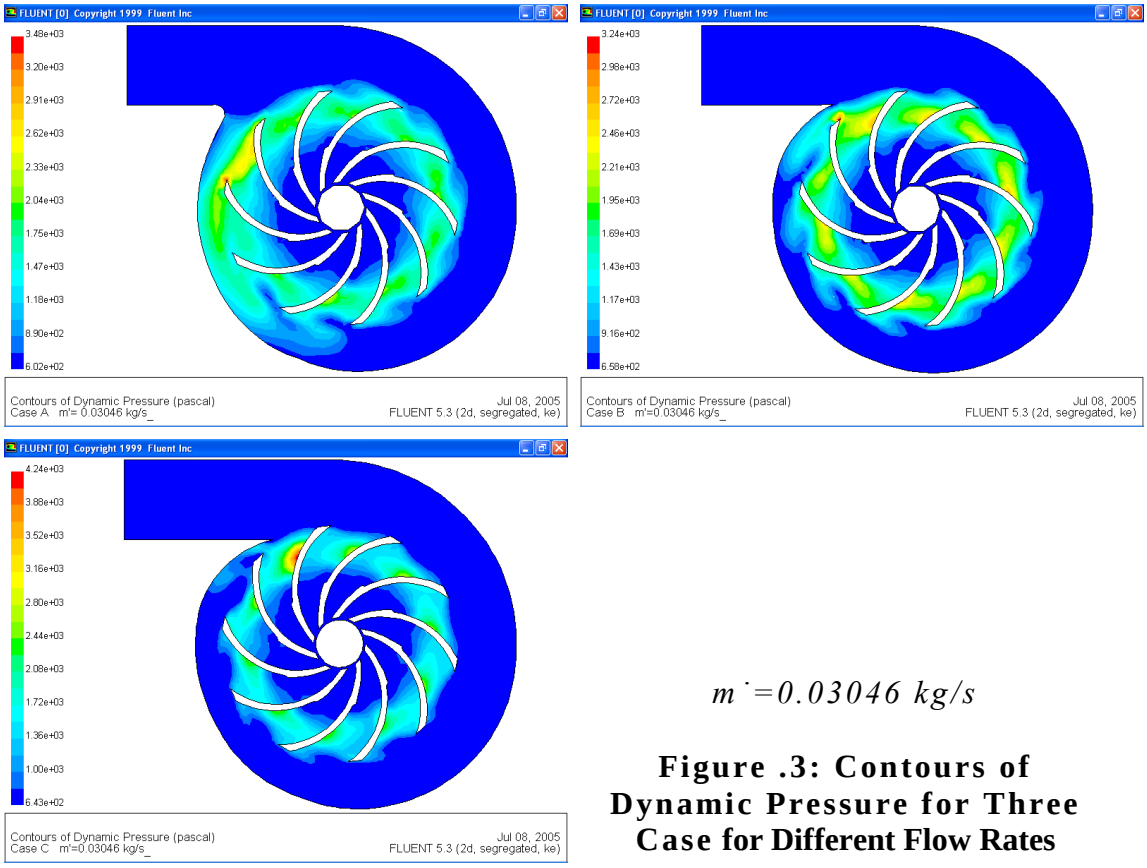

$\dot{m} = 0.03046\ kg/s$

Figure .3: Contours of Dynamic Pressure for Three Case for Different Flow Rates

2. EXPERIMENTAL APPARATUS AND ANALYSIS TECHNIQUES

Figure.4: Test Rig View

2.1. Experimental Apparatus

The fan used in this study is a single-stage machine with an unshrouded impeller and external volute. The test rig has been constructs to form an open loop system, as shown in the Figure (4). The loop consisted of a constant-speed electric motor, a throttle valve, a metering orifice, and piping. A scroll (volute) of square cross sectional area collects the air. The outlet pipe of the fan is connected to an orifice plate air flow meter through 25 cm length flexible pipe. The throttle valve (gate valve), fitted

on the discharge side of the piping, and allows an accurate and fine control of the mass flow rate. A 0.6 kW, 220-v AC motor that has a constant rotational speed of 16000 rpm, directly drives the fan. The whole assembly is mounted on a heavy specially constructed wood structure. The impeller used for the test fan is an unshrouded type, as shown in Figure (5). It is fitted on the rotating shaft, which is directly connected to the motor. The blades of this impeller are of backward shape having a thickness of (3mm). The details of the impeller technical data are shown in Table (2).

Table 2: Fan Technical Data

Impeller exit diameter (D_1=110 mm)
Impeller inlet diameter (D_2=34 mm)
Number of impeller blades (Z=10)
Speed(Ω_2=16000 rpm (U2=1675.52 m/s)
Inlet blade angle (β1= 54°)
Inlet blade angle (β2=42°)
Blade thickness (t = 3mm)
Discharge width (b_2= 25 mm)
The gap between the tongue and the impeller (Case A=12.76mm,Case B=7.2 mm , Case C≈0 BB=7.2mm Case C≈0.0)

'igure.5:Impeller View

2.2 Volute designs and measurement Location

The collecting volute which is part of the centrifugal fan, it is a fully integrated part of the case and its cover. Three volute tongue designs are investigated. In type A, the leading edge of the tongue is rounded, in type B, the tongue is cut back, allowing for flow recirculation. Finally, type C, where a full tongue is used, it is almost impossible for the air to recirculate ar The details of the gap between the volute tongue and the impeller for three volute tongue configuration are shown in Table (2) and Figure (6).The measurements for the present study are carried out on the front-wall of the fan casing. Several measurement taps are arranged on this wall, as shown in Figure (2). These taps are distributed on radial and angular positions, as follows;

1. Eight taps are arranged along a radial path at angular position of 60° on the shroud.
2. Eleven taps are arranged along a radial path at angular position of

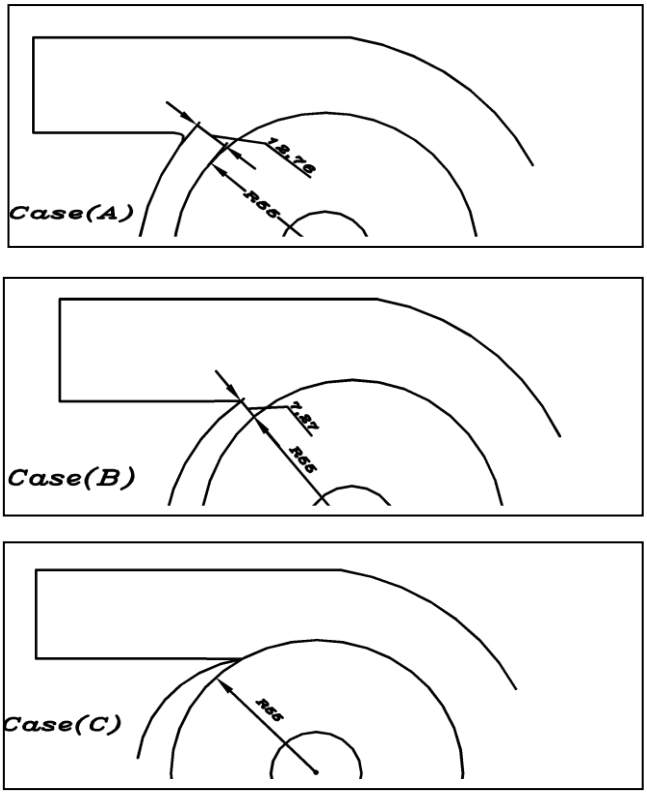

Figure.6: The Gap between The Volute Tongue and the

240° on the shroud wall and volute casing. The distance between every consecutive taps is taken as 5 mm for all the previously mentioned path arrangements.
The angular position Ø is zero at the edge of the tongue and it increases with anti-clockwise orientation, as shown in Figure (7).
3. Twelve taps are located at every 30° interval around the front side of the volute, and at location of 5 mm from the outlet of the impeller.
4. Ten taps are located every 30° interval around the volute casing, at the center of casing width.

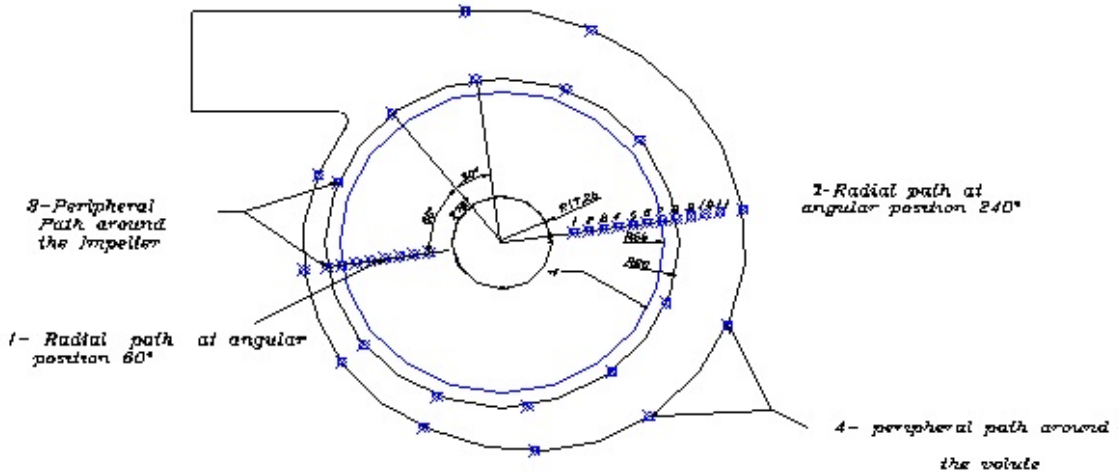

Figure .7: Locations of Measuring Points

2.3. Instrumentation and Analysis Techniques

Stainless steel tubes of 1 mm diameter and 15 mm length are constructed to be used as pressure taps in this study. The tubes are inserted into the holes (which are drilled on the front side of the fan casing), perpendicularly to the casing wall until the pressure hole of the tube reaches the surface of the casing wall. The other end of the tube is extended out of the other side of the fan casing. A short plastic tube is employed to connect the transducer of the pressure tap. The static pressure measurements are carried out, by employing a piezoelectric (-0.3 to 0.3) bar, which corresponds to an output voltage of (-5 to 5) volt of the transducer. The output signals from the transducer are appropriately conditioned and digitized using the data acquisition system. This techniques are based on evaluating the voltage output of the transducer at equally interval of time, so that , a record of voltage values is obtained and stored in computer memory for further processing. The output signals are also connected to an oscilloscope, to monitor the onset of any perturbation in the flow. This observation will give a continuous display of the variation and measurement problems in order to avoid it.

Comparison with Experimental Data

The results of the numerical simulation were recorded for the same locations considered in the experiments. The static pressure distributions around the volute for three cases (A, B, C) for three mass flow rates are compared in Figure (8). Agreement between the numerical and experimental data is good, although the numerical result is obtained for a complete revolution of the impeller and the experimental is an instantaneous measurement.

Some differences have arisen in the comparison between the numerical and experimental static pressure in the volute of the tested centrifugal fan, especially near tongue region. Also, from this comparison it can be concluded that, the accuracy of the prediction of the circumferential pressure distribution is better at lower flow rate, which leads to the assumption that the intensity of the dynamic pressure is a source of inaccuracy in the calculation.

3. Discussion of Results

The static pressure and pressure fluctuations at different points on the centrifugal fan casing are determined by water monometer or by the output of the pressure transducer. The mass flow rate values which are used in the resent study cover the values, nearly non-flow , 0.0091 kg/s, 0.0168 kg/s, 0.023 kg/s, 0.03046 kg/s. These values are chosen arbitrarily but the maximum value of the mass flow rate (0.03046 kg/s) is limited by the control valve and fan design.

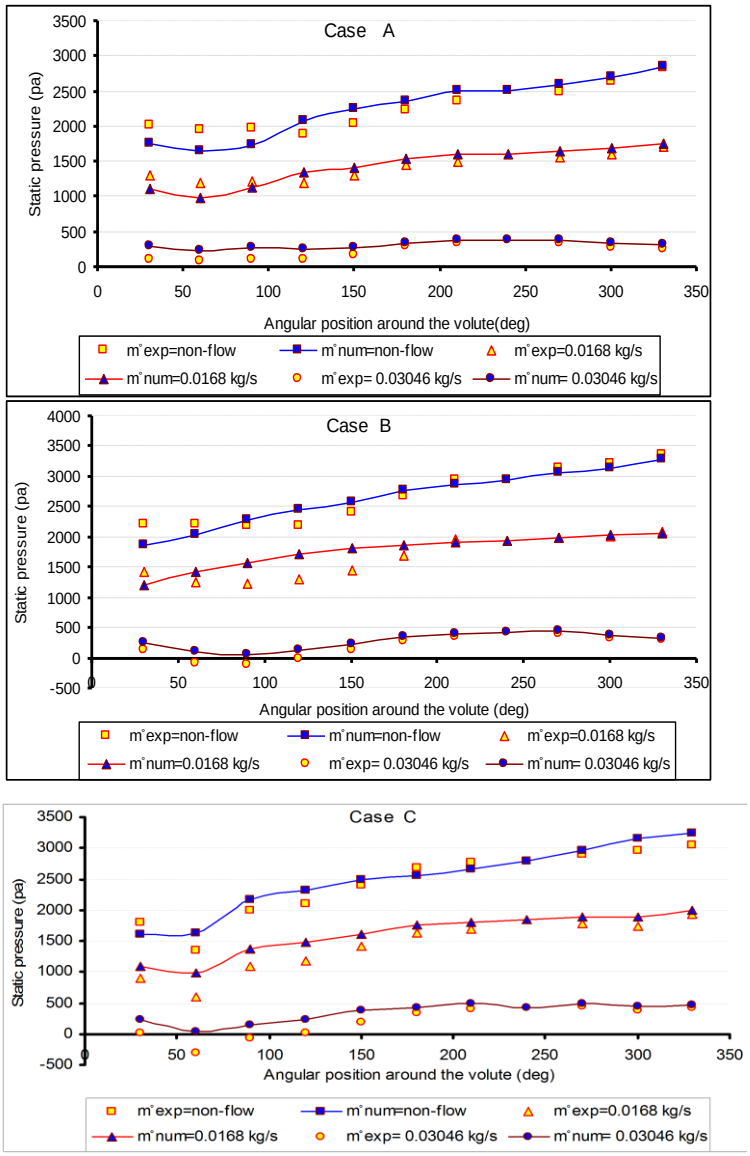

Figure .8: Comparison of the static pressure around the volute for three cases

3.1Overall Performance and Static Pressure Measurements

Figure (9) show the difference between the performance map of the fan for the three cases (A , B , and C) , which is larger at lower mass flow rate , but these differences disappear as flow rate is increased . At the low flow rates, cases A and B provide an improved pressure compared with that for case C.

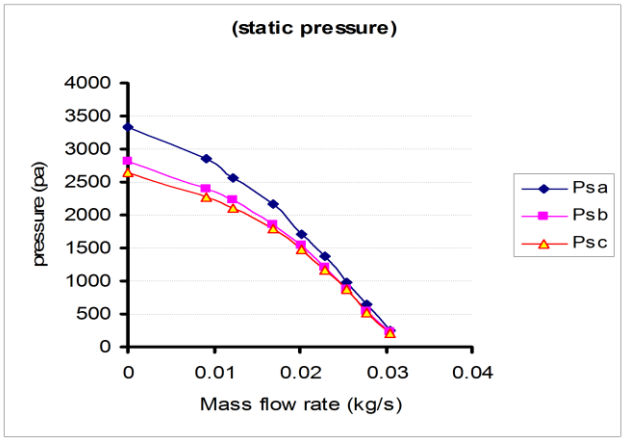

Figure.9: Performance Characteristics

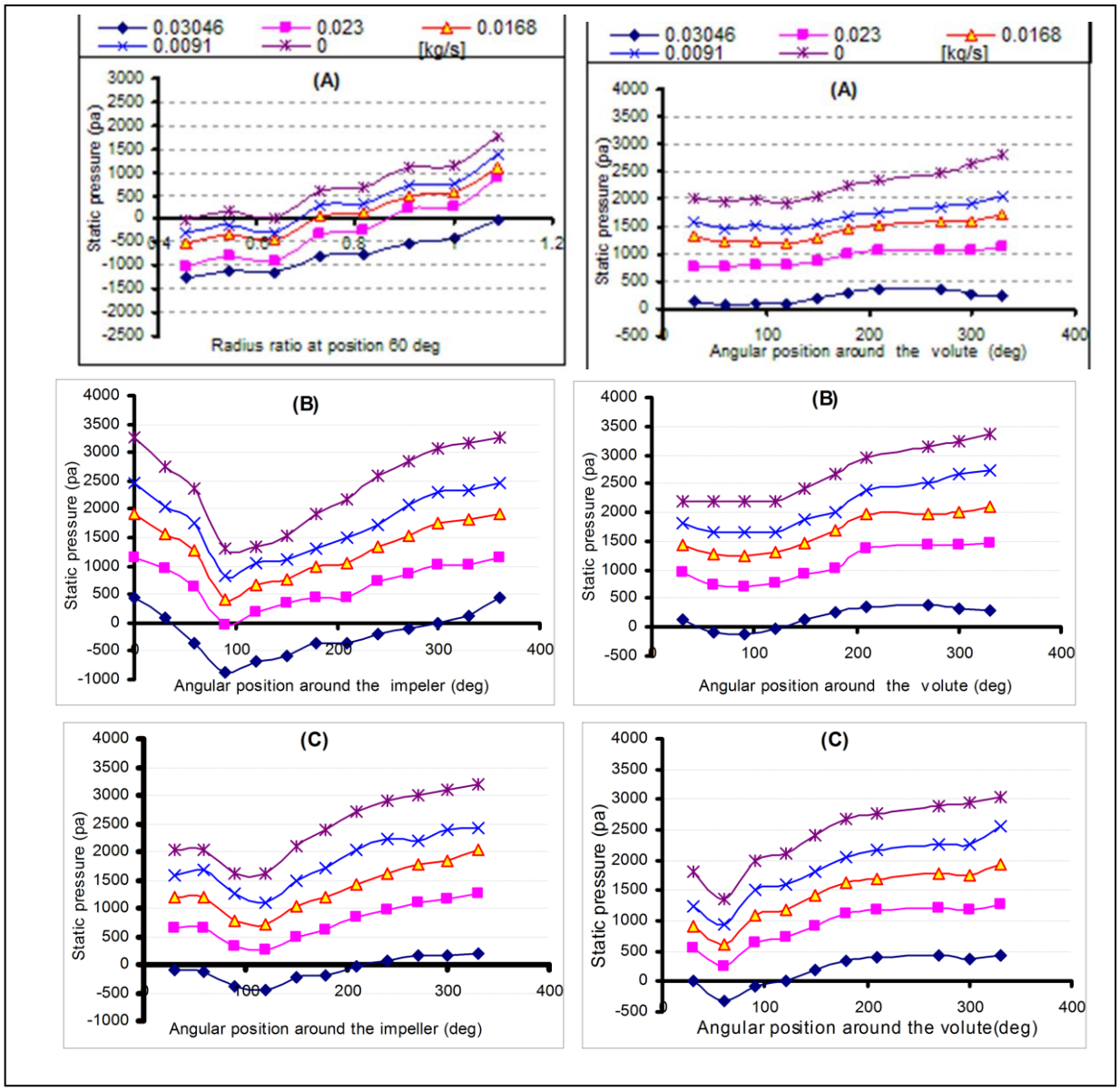

Figure (10) show the distribution of the static pressure along the

Figure .10: Circumferential Static Pressure Distribution around the impeller and volute for Several Values of the Flow Rate for Three Cases (A, B, C)

periphery of the impeller and volute for various flow rates. It can be indicated that the pressure distribution for the design mass flow rate (i.e. mass flow rate = 0.03046 kg / s), will

produce a fairly constant pressure distribution. Around the impeller ,for mass flow rate which is less than standard , the static pressure gradually decreases beyond the tongue in the direction of flow to about angular position (Ø = 120^{o}) depending on the case (A,B , and C) ,whereas, between Ø=120^{o} and the volute outlet, the opposite will occur.

This is because the volute area decreases from the tongue region toward position at Ø=120^o and increases after that .The velocity or pressure head of the flow will be converted to the other one. The figure also shows that static pressure around the volute increases as the angular position increases except at position Ø = 60^o for case C , where a separation eddy exists downstream of the leading edge of the tongue C and it is not observed with volute designs A and B. This result agrees with that result obtained by Whitfield et al. (11).
Figure (7) show the pressure distribution along the shroud at angular position Ø = 60^o and 240 ^{o} for various mass flow rates for three cases (A, B, and C). As indicated from this figure , the static pressure gradually increases as the radius ratio increases until the radius ratio reaches the value of ($r / r_I = 1.091$) (at angular position 240^o), where the rate of pressure rise is decreased. This is due to the end of the diffusion in the volute region. Also, the static pressures for all radius ratios at position Ø = 60^o have lower values than those at position Ø=240^o.This phenomenon is due to a non uniform pressure distribution around the impeller which results from volute design .This non uniform pressure distribution extends upstream to the impeller inlet and hence influences the flow through the impeller.

3.2 Pressure Fluctuation measurements

Figure (11) shows the pressure fluctuations in the time domain over a period of 60 ms for various mass flow rates at angular position Ø=30° (beyond of the tongue) for three cases. It is clear from a figure that as the mass flow rate is reduced, the pressure fluctuations amplitude increases. The maximum pressure fluctuations amplitude occurs at mass flow rate equal to nearly non-flow and 0.0091 kg/s. At mass flow rate higher than 0.0091 kg/s, the pressure fluctuations have minimum amplitude and they seem to be nearly steady. The figure also shows that, the pressure fluctuations for various mass flow rates are non-periodical in nature .In general; the pressure traces do not show any distinct periodic fluctuations. The power spectrum plots which correspond to the pressure fluctuations for various mass flow rates at angular position Ø=30° for three cases, are represented in Figure (9). The plot demonstrates the broad band component (from 0 Hz to about 500 Hz) which is a manifestation of the higher level of random frequency of pressure fluctuation for various mass flow rates. These observations are applicable to all locations of fan casing and for three cases (A, B, and C). It can be concluded that the fan does not stall until the mass flow rate is reduced to very small values .This result agrees with that result obtained by (Kinoshits and Senoo, 1985) and (Saad, 2000), who found that the fan without the diffuser is stable at all operating conditions.

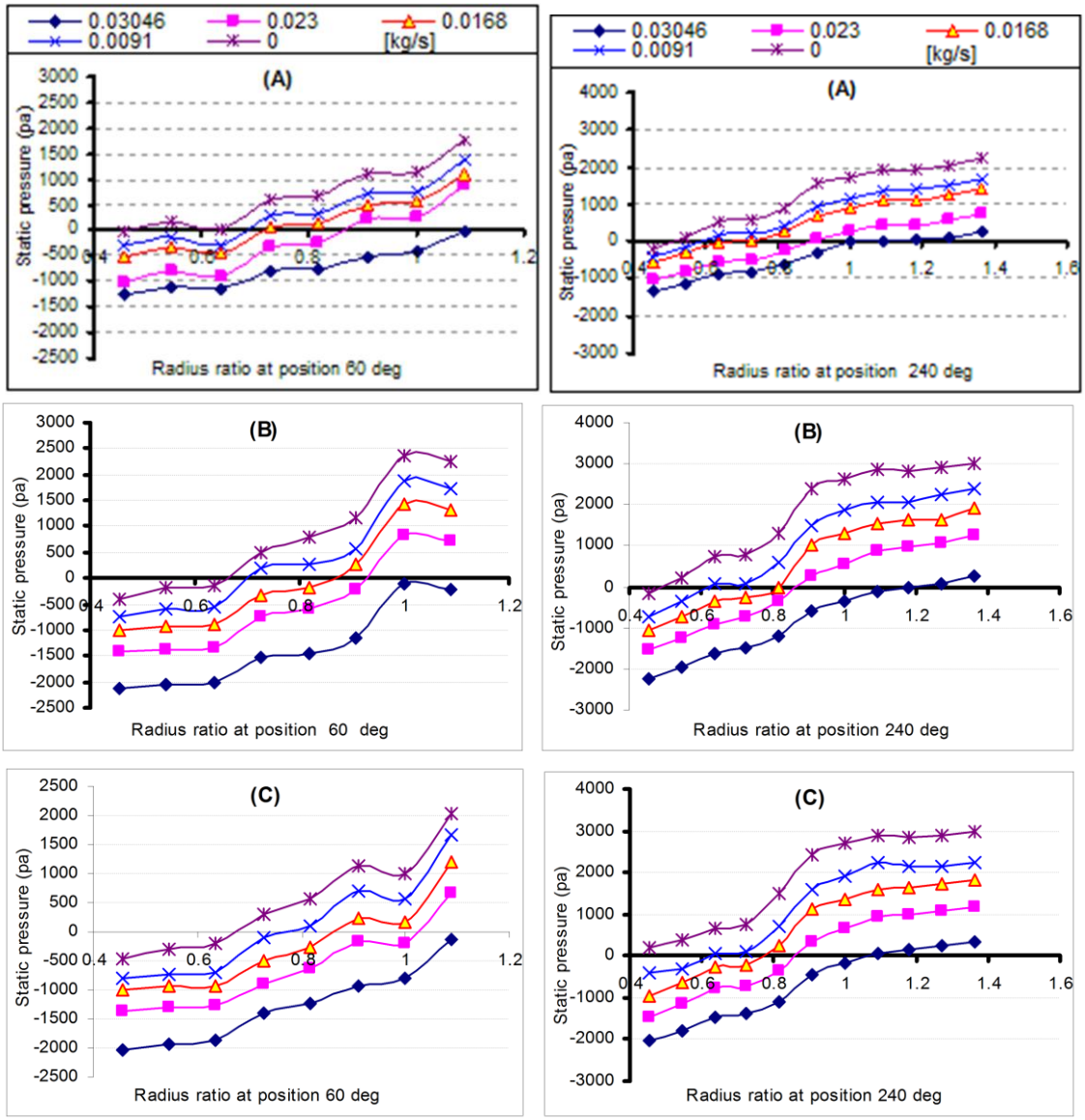

Figure.11: Variation of Static Pressure with Radius Ratio at Position 60° and 240° for Various Mass Flow Rate for Three Cases (A,B,C)

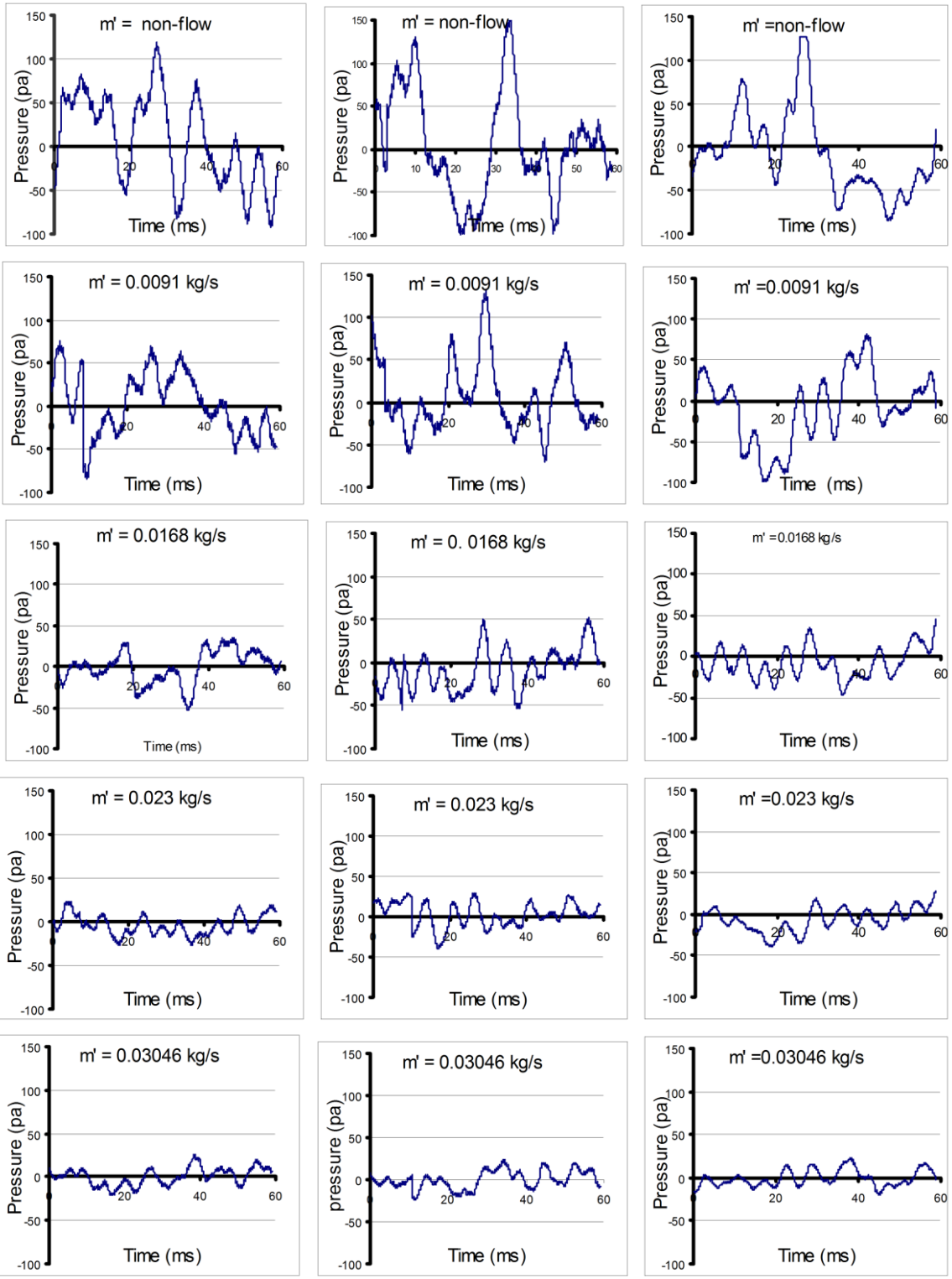

Case (A) Case (B) Case (C)

Figure.12: Pressure Fluctuations in the Time Domain Measured at Angular Position Ø=30 ° for Various Mass Flow Rate (Three Cases).

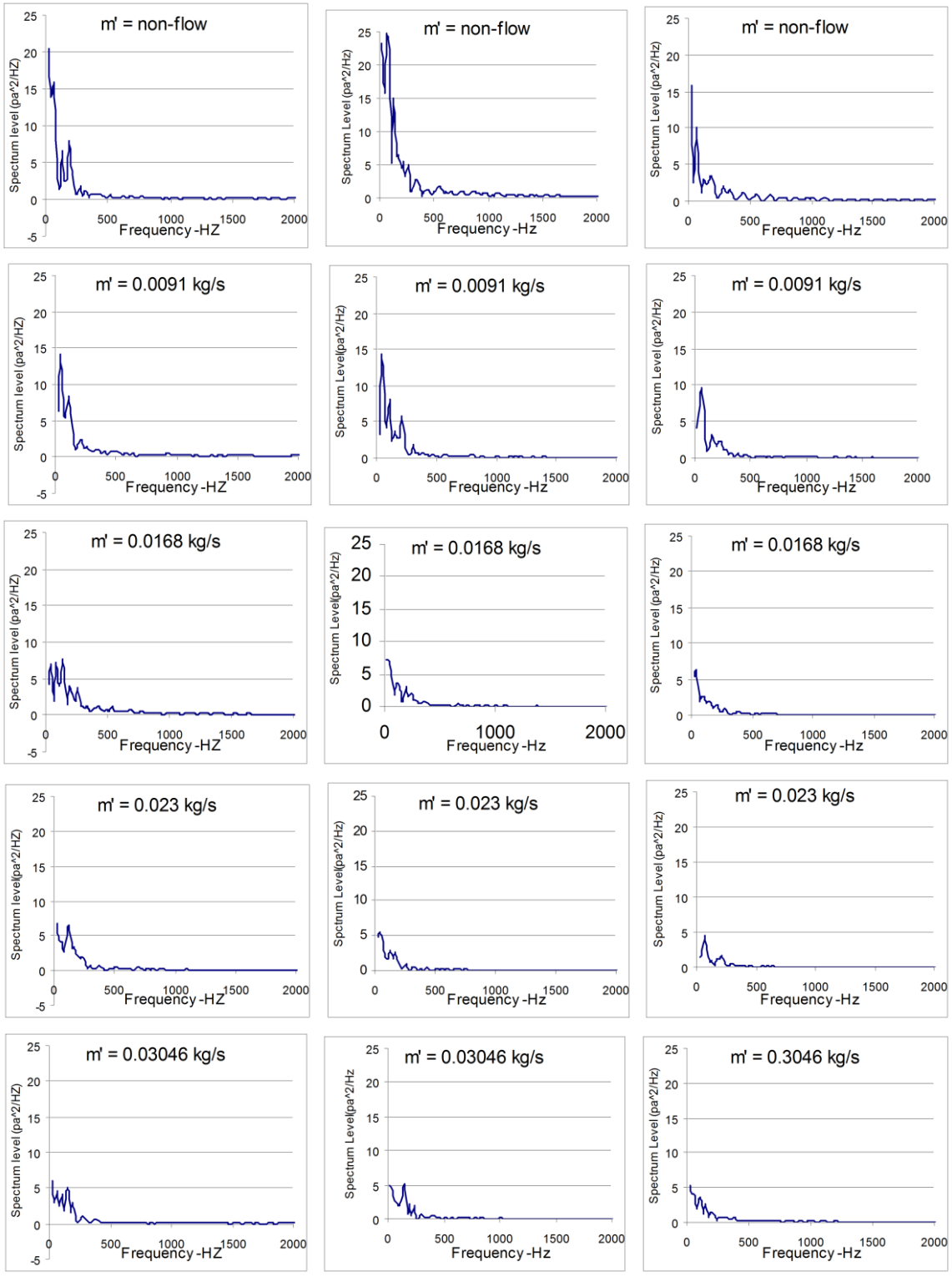

Fiqure.13: Power Spectrum of Pressure Fluctuations Measured at Angular Position Ø=30 ° for Various Mass Flow Rates (Three Cases).

3.3 Strength of the Pressure Fluctuations measurements

Figure(14) shows the distribution of the strength of pressure fluctuation around the impeller and volute for several values of flow rate for cases (A , B , and C) . It can be indicated that the pressure fluctuation around the impeller has maximum values for mass flow rate = non-flow and mass flow rate = 0.0091 kg/s at all positions for case C. At all flow rates , for case B , the pressure fluctuation has a maximum value at position $\emptyset = 30^{o}$ (beyond the tongue) and the strength is very small at other positions . This phenomenon occurs because of the switching in the flow direction between the recirculation duct and the discharge duct. This result agrees with the result obtained by (Whitefield et al., 2000). Case A has a maximum strength at positions ($\emptyset = 0^{o}$ and 150^{o}) for nearly non – flow and $\dot{m} = 0.0091$kg /s.

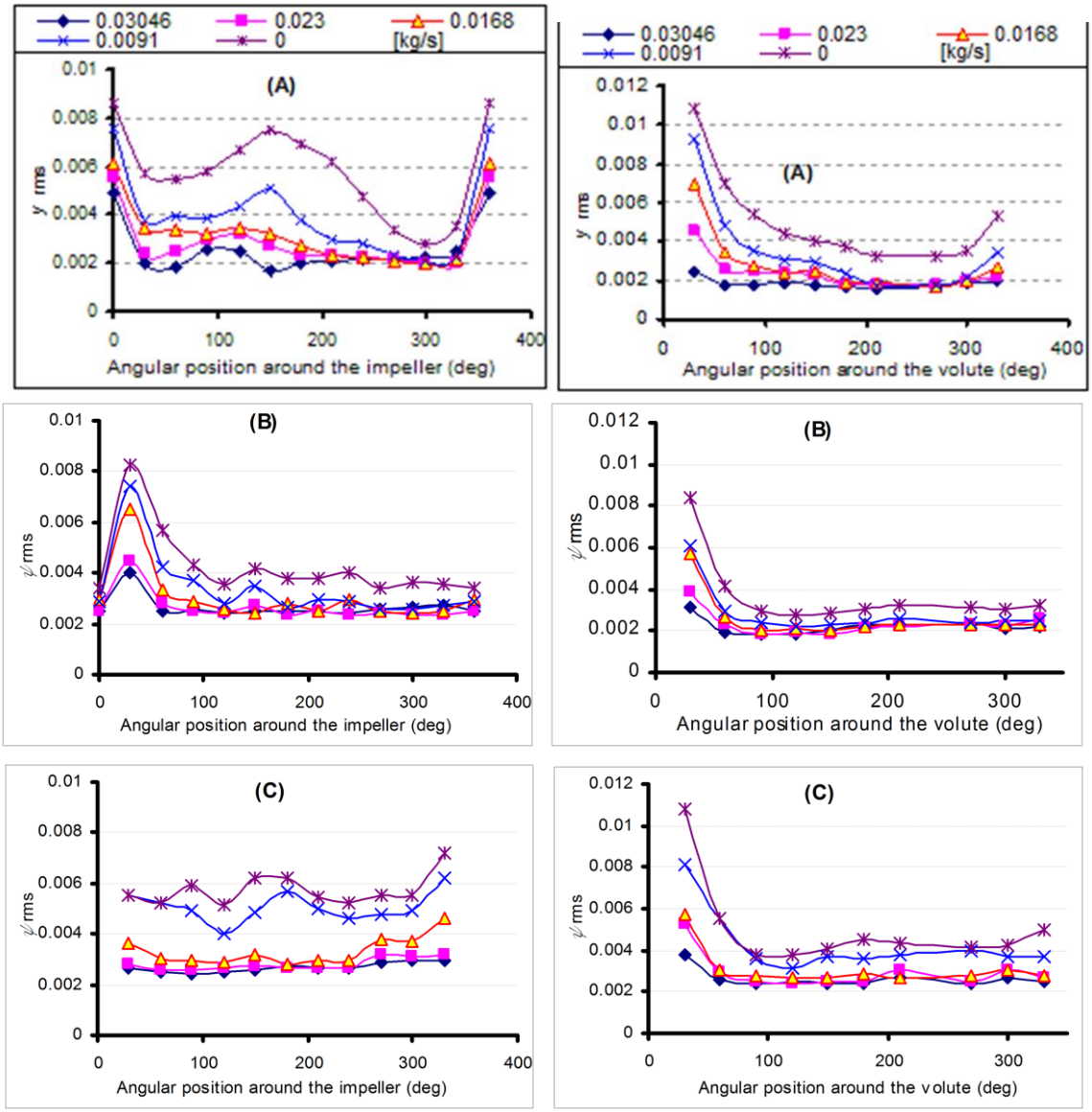

Figure.14: Distribution of Strength of Pressure Fluctuation around the Impeller and volute for Several Values of the Flow Rate for Three Cases (A, B, C).

Also, for each rate , the strength of pressure fluctuation around the volute is maximum at Ø = 30° and is nearly constant at other positions toward the volute exit . The collecting volute of centrifugal fan when operating at off – design condition (i.e. Q = non flow), produces a peripheral static pressure distortion around the impeller (Figure (10)).

This pressure distortion intensively acts back on the impeller exit and leads to a periodic throttling of the impeller flow. This results in a cyclic acceleration and deceleration of the air inside each impeller channel and increases the pressure fluctuation around the impeller (10).

The radial distribution of strength of pressure fluctuation at position Ø = 60° and Ø = 240° for various flow rates and the three cases can be seen in Figure (15). As shown in this figure , the maximum pressure fluctuation at position Ø = 60° is Flow

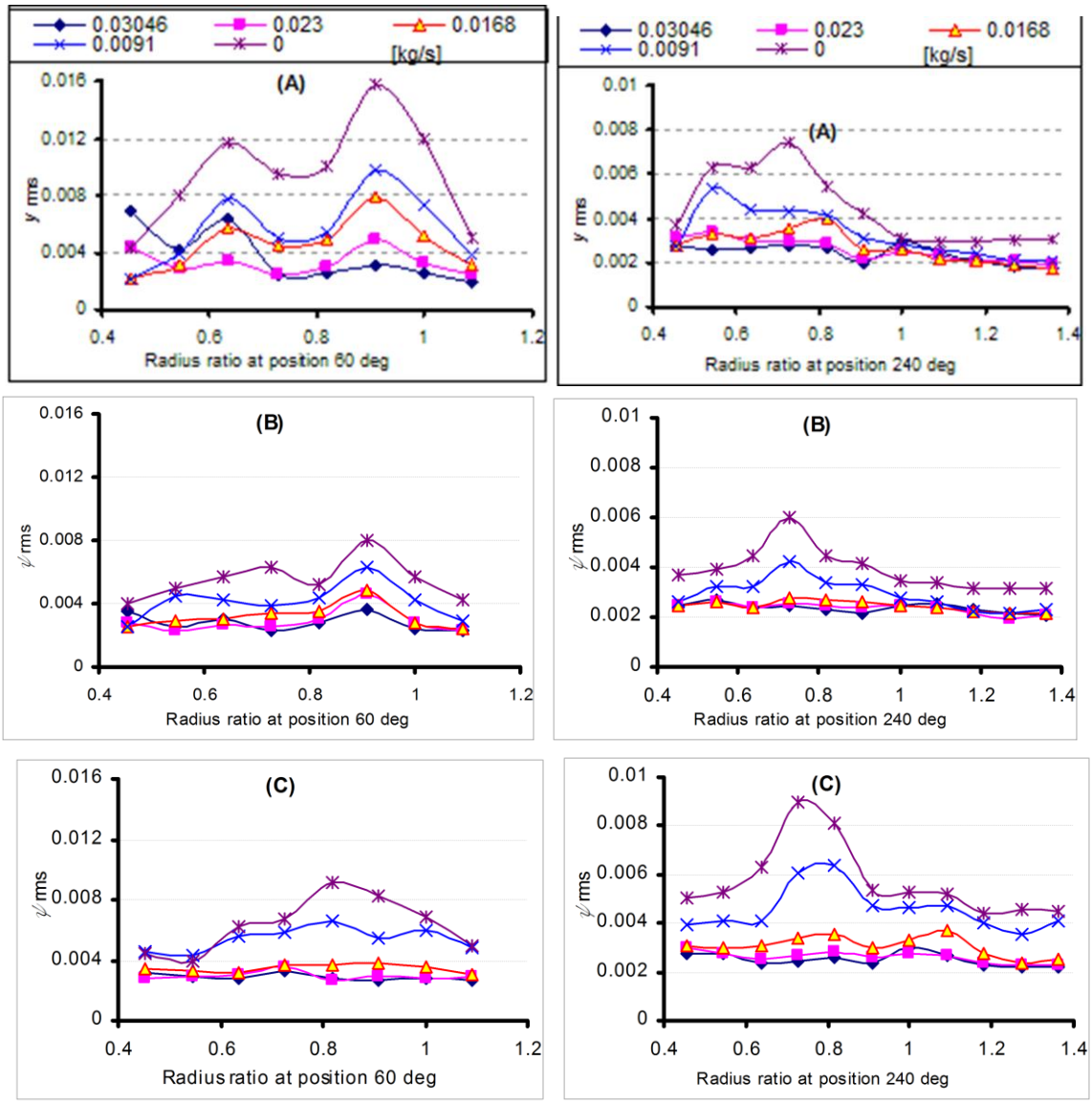

Figure.15: Variation of the Strength of Pressure Fluctuation with Radius Ratio at Position 60 ° for Various Mass Flow Rates.

Observed at radius ratio (r / r_I = 0.909) for two cases (A and B). While for case C it is indicated at radius ratio r/r_I = 0.818. The pressure

fluctuation at position Ø = 240^o for the three cases is higher at radius ratio r/r_I = 0.727, and case C has higher pressure fluctuation than cases (A and B) .This figure also shows that at radius ratio higher than (r/r_I >1), the pressure fluctuation is nearly constant

CONCLUSIONS

1. The impeller – volute interaction in the centrifugal fan is successfully predicted by a numerical model using finite volume commercial code. The qualitative numerical data analysis shows that the main flow phenomena are adequately simulated: static and dynamic pressure variation around the volute and impeller, changes with flow rate .
2. Agreement between the numerical and experimental static pressure data in the volute is fairly good; some differences have arisen, especially near tongue region and at higher flow rate.
3. The unsteady calculation combined with the moving reference frame technique has proved to be a good tool to investigate the impeller – volute interaction.
4. The pressure fluctuation for various mass flow rates is non-periodical nature, as the mass flow rate is reduced, the pressure fluctuation amplitude increases.
5. The higher level of random frequency of pressure fluctuation for various mass flow rates is manifested as the broad band components (from 0 Hz to about 500 Hz).
6. The pressure fluctuation strength value around the volute for three cases (A,B and C) is maximum at Ø = 30^0 and is nearly constant at other position toward the volute exit.
7. The maximum pressure fluctuation in the radial direction for various flow rates and three cases is observed at radius ratio before the trailing edge of blades of the impeller (from r/ri = 0.727 to r/ri = 0.909).

REFERENCES

[1] Brennen, C. E. 1994. Hydrodynamics of Pumps, Oxford University Press, and CETI Inc.

[2] Dong, R. Chu S. Katz, J. 1997. Effect of Modification to Tongue and Impeller Geometry, on Unsteady Flow, Pressure Fluctuations, and Noise in a Centrifugal Pump. ASME Journal of Turbomachinery., 119 : 506–515.

[3] Rolling, R. E. Carlson, J. J. Iversen, H. W. 1960. Volute Pressure Distribution, Radial Force on the Impeller, and Volute Mixing Losses of a Radial Flow Centrifugal Pump. ASME Journal of Engineering for Power : 136-144.

[4] Kaupert, K. A. Staubli, T. 1999. The Unsteady Pressure Field in a High Specific Speed Centrifugal Pump Impeller. Part I: Influence of the Volute. ASME J. of Fluids Engineering, 121 : 621–626.

[5] Whitfield, A. Hamada, M. Sakai, T. Tsujit, S. 2000. Flow measurement around a fan volute tongue using particle tracking velocimetry. Proc. Inst. Mech.. Eng., Vol. 212, Pt A : 235-246.

[6] Parrondo, J. L. Ferna´ndez, J. Gonza´lez, J. Ferna´ndez, L. 2000. An Experimental Study on the Unsteady Pressure Distribution around the Impeller Outlet of a Centrifugal Pump. ASME-FEDSM-00-11302.

[7] Hagelstein, D. R. Keiper, Van Den Braembussche, R. 2000. Experimental and Numerical Investigation of the Flow in a Centrifugal Compressor Volute. ASME Journal of Turbomachinery, Vol. 122 : 22-30.

[8] Croba, D. Kueny, J. L. 1996. Numerical Calculation of 2D, Unsteady Flow in Centrifugal Pumps: Impeller and Volute Interaction. Int. J. Numerical Methods Fluids, 22 : 467–481.

[9] Blanco, E. Ferna´ndez, J., Gonza´lez, J. Santolaria, C. 2000. Numerical Flow Simulation in a Centrifugal Pump with Impeller-Volute Interaction. ASME-FEDSM-00-11297.

[9] Gonza´lez, J. Blanco, E. Ferna´ndez, J. Santolaria, C. 2002. Numerical Simulation of the Dynamic Effects Due to Impeller-Volute Interaction in a Centrifugal Pump. ASME Journal of Fluids Engineering, Vol. 124: 348-355.

[11] Lakshminarayana, B. 1991. An Assessment of Computational Fluid Dynamic Techniques in the Analysis and Design of Turbomachinery. The 1990 Freeman Scholar Lecture, ASME J. 0f Fluids Eng.. Vol.. 113 : 315–352..

The work was carried out at the college of Engineering. University of Kirkuk